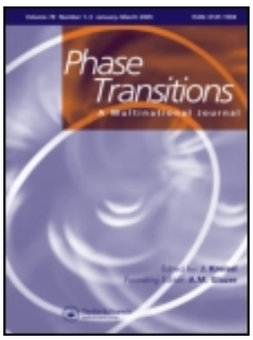

Taylor & Francis
Taylor & Francis Group

Phase Transitions
A Multinational Journal

ISSN: 0141-1594 (Print) 1029-0338 (Online) Journal homepage: https://www.tandfonline.com/loi/gpht20

Electrical, optical and fluorescence percolations in P(VAc-co-BuA)/MWCNT composite films

Ertan Arda , Selim Kara & Önder Pekcan

To cite this article: Ertan Arda , Selim Kara & Önder Pekcan (2013) Electrical, optical and fluorescence percolations in P(VAc-co-BuA)/MWCNT composite films, Phase Transitions, 86:10, 1017-1032, DOI: 10.1080/01411594.2012.751535

To link to this article: https://doi.org/10.1080/01411594.2012.751535

Phase Transitions, 2013
Vol. 86, No. 10, 1017–1032, http://dx.doi.org/10.1080/01411594.2012.751535

Electrical, optical and fluorescence percolations in P(VAc-co-BuA)/MWCNT composite films

Ertan Arda[a]*, Selim Kara[a] and Önder Pekcan[b]

[a]*Department of Physics, Faculty of Science, Trakya University, 22030 Edirne, Turkey;* [b]*Faculty of Arts and Science, Kadir Has University, 34320 Cibali, Istanbul*

(*Received 27 August 2012; final version received 16 November 2012*)

Effects of multiwall carbon nanotube (MWCNT) addition on the electrical conductivities, optical transparencies and fluorescence emissions of poly(vinyl acetate-co-butyl acrylate) (P(VAc-co-BuA))/MWCNT composite films were studied. Optical transmission, fluorescence emission and two point probe resistivity techniques were used to determine the variations of the optical, fluorescence and electrical properties of the composites, respectively. Transmitted photon intensity (I_{tr}), fluorescence emission intensity (I_{fl}) and surface resistivity (ρ_s) of the composite films were monitored as a function of MWCNT mass fraction (M) at room temperature. All these measured quantities of the composites were decreased by increasing the content of MWCNT in the composite. The conductivity and the optical results were attributed to the classical and site percolation theories, respectively. The fluorescence results, however, possessed both the site and classical percolation theories at low and high MWCNT content regions, respectively.

Keywords: poly(vinyl acetate-co-butyl acrylate); multiwalled carbon nanotube; percolation; critical exponents; conductivity; fluorescence

1. Introduction

Poly(vinyl acetate) (PVAc) is a non-crystalline, amorphous thermoplastic polymer. The PVAc is generally fabricated *via* mixing process with certain polymeric materials in order to reinforce the structural properties [1,2]. PVAc-based composites are widely used in adhesive, paper, emulsifier, paint and textile industries due to its high-bond reinforced, film-like, nonflammable and odorless characteristics [2]. Furthermore, because of their high dielectric constant values and high dielectric strengths, the PVAc could be used as a good gate insulator for organic film transistors [3]. P(VAc-co-BuA) is one of the most important industrial latexes, widely utilized in water-based architectural (exterior or interior) coatings, and adhesives market, is the vinyl acetate (VAc)/butyl acrylate (BuA) emulsion copolymer [4,5] with a BuA composition of 15–30%, since they have higher mechanical and water resistance properties than the homopolymers of both monomers.

After the carbon nanotubes (CNTs) discovered by Iijima, polymer/CNT composite studies were first reported by Ajayan et al. [6]. CNTs and polymer-composites having

*Corresponding author. Email: ertana@trakya.edu.tr

CNTs are used in various industrial applications such as flat panel screens, electron microscope guns, gas discharge tubes, microwave amplifiers, fuel cells, batteries, hydrogen storing media, nanoprobes, sensors and body-parts of aircrafts and spacecrafts [7]. It has been well known that some CNTs are stronger than steel and lighter than aluminum and more conductive than copper [7]. Studies on polymer/CNT composites have been of interest at last decade. There are two main types of CNT known as single (SWCNT) and multiwalled (MWCNT). Thermoplastic polymers are usually used as an insulating material because of their low electrical conductivity properties ($\approx 10^{-15}\,S\,m^{-1}$). By doping the conducting fillers such as carbon black (CB) and CNT into polymer matrix forms highly conductive polymer composites. The electrical resistivities of polymer/MWCNT composites may vary between 10^{16} and several ohms. The electrical resistivities of polymer/CNT composites are strongly dependent on the volume or mass fractions of the doped CNTs. At low volume or mass fractions, the resistivity remains very close to the resistivity of the pure polymer. However, by addition of some CNTs, above a critical concentration (known as percolation threshold) insulating polymers become conductive composites. If CNTs in the polymer matrix form a conducting network, the conductivity of composite dramatically increases. This phenomenon is called as percolation and can be well explained by percolation theory [8]. Percolation threshold can be usually determined by monitoring of resistivity variations in composites. Electrical percolation thresholds for some MWCNT and SWCNT polymer-composites were reported as ranging from 0.0021 to 15 wt% [9]. It has been shown that the electrical, mechanical, and thermal properties of polymer/CNT composites can be improved by addition of CNTs [9–11].

There are plenty of studies about conducting PVAc composites in the literature. Wang et al. [12] produced conducting PVAc-nanocomposite fibers with functionalized MWNTs which were produced by oxidation technique and unfunctionalized MWNTs by using electrospinning method. They measured conductivity of a single nanofiber by two-probe method. They found that increasing the mass fraction of MWNT also increases the conductivity showing a percolative behavior, and the percolation threshold was obtained around 0.5 wt%. The effect of clay as a secondary filler on emulsion-based and solution-based CB-PVAc composite films were investigated by Miriyala et al. [13], where the percolation threshold of emulsion-based composite films were found to be lower than the solution-based PVAc films. Furthermore, the addition of 0.2 wt% clay in composite structure leads to decrease in the electrical percolation threshold and increase in the storage modulus. Grunlan et al. performed a large amount of studies about the electrical and thermal conductivities of the PVAc composites [14–19].

Recently, film formation from PVAc latex particles [20–22], electrical and optical percolation properties of polystyrene/MWCNT composites [23] were studied by our group. In this current work, the effect of MWCNT addition in insulating PVAc matrix was investigated. Variations in electrical, optical, and fluorescence properties of P(VAc-co-BuA)/MWCNT composite films were measured by using two-probe surface resistivity, photon transmission, and fluorescence emission measurement techniques. The electrical, optical, and fluorescence percolation thresholds were determined. The classical and site percolation theories were used to calculate the critical exponents for the surface resistivity and for other two data sets, respectively. Percolation models and critical exponents for fluorescence emission data were found to be in accord with the optical and electrical data at low and high MWCNT content regions, respectively.

2. Experimental

2.1. *Preparation of the P(VAc-co-BuA) latex particles and the composite samples*

VAc and BuA (85 : 15 wt%) were used to synthesize the waterborne P(VAc-co-BuA) latex particles by emulsion polymerization technique [24]. The average particle size and glass transition temperature of the PVAc latices were found to be 245.5 nm and 31.3°C, respectively. In the rest of this article, the term PVAc will be used instead of the term P(VAc-co-BuA) in order to simplify the reading.

MWCNT (Aldrich 659258) with outer diameter of 110–170 nm and length of 5–9 μm was used to prepare the composites. Purity of the MWCNT is reported as minimum as 90% and it was used without any further purification process. Poly(vinyl pyrrolidone) (PVP40, Sigma-Aldrich) was used as dispersion agent of MWCNTs in the water. Physical association of polymers with CNT surfaces was shown to enhance the dispersion of CNT in both water and organic solvents [25,26]. One of the suggested mechanisms is "wrapping" [26], which is believed to rely on specific interactions between a given polymer and the tubes. For example, the reversible association of SWNT with linear polymers, PVP and polystyrene sulfonate, in water was identified as being thermodynamically driven by the elimination of a hydrophobic interface between the tubes and the aqueous medium [26]. Among the widely used polymers for this purpose PVP has been identified as one the best of wrapping functionalization of tubes and already used to disperse or stabilize CNTs in aqueous environment [27].

Firstly, PVAc (4% w/v) – water dispersion with pyranine(P) (8-hydroxypyrene-1,3, 6-trisulfonic acid trisodium salt, Fluka 56360) (2×10^{-4} M) as a fluorescence probe was stirred by a magnetic stirrer for 24 h. Since, the van der Waals forces between MWCNTs prevent homogeneous distribution of the nanotubes in water then, PVP was added to dispersion with a concentration of 5 mg mL^{-1} to separate the MWCNTs from each other. This dispersion was splitted into 15 different containers. The PVAc/MWCNT dispersions with 14 different MWCNT content were prepared in these containers by varying the MWCNT concentrations and stirring them for 12 h. A pure (non MWCNT content) dispersion was also prepared. Mass fractions of PVAc/MWCNT dispersions were calculated as

$$M = \frac{m_{\mathrm{MWCNT}}}{m_{\mathrm{MWCNT}} + m_{\mathrm{PVAc}}} \tag{1}$$

where, m_{PVAc} and m_{MWCNT} are the masses of the PVAc and MWCNT in the dispersions, respectively. Mass fractions of the composites were obtained by using Equation (1); 0, 0.5, 1.0, 1.3, 1.6, 1.9, 2.2, 2.7, 3.2, 4.0, 5.0, 7.0, 10, 13 and 18 wt%, respectively. Composite films were prepared from PVAc/MWCNT dispersions by placing same number of drops by using a micropipette on 2.5×3.0 cm^2 glass plates and allowing the water to evaporate at room temperature. It was observed that, the dried pure PVAc (non-MWCNT content) composite film was optically transparent due to low glass transition temperature (T_g) values of the latex, i.e., the film formation process was completed at room temperature. Figure 1 shows a cartoon representation of the film cross-section with distribution of latex-particle boundaries before and after the film formation processes is completed. Glass plates of the samples were weighed before and after the composite film casting to calculate the film thicknesses. The average film thickness was determined as 21.5 μm.

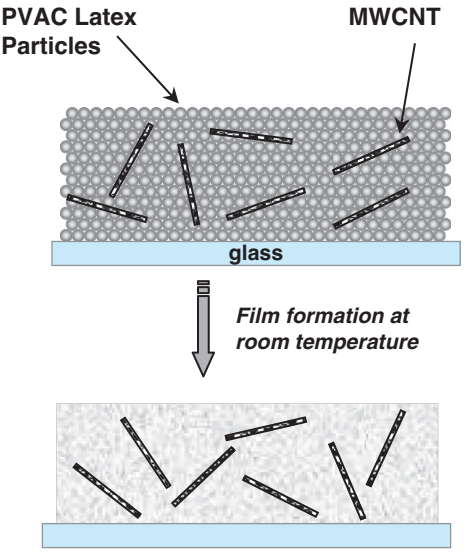

Figure 1. The cartoon representation of the film cross-section before and after the film formation.

2.2. *Optical transmission, fluorescence emission and resistivity measurements of the composites*

UVV spectrophotometer (Lambda 2S of Perkin–Elmer, USA) was used to monitor the variation of optical transparency of the composite films. Since the absorbance region of the pyranine molecule was 300–430 nm, the transmittances of the composite films were detected at 470 nm wavelength. Transmission measurements were performed at six different positions on the film surface in order to lower the error. Thus, the average value of transmitted light intensity (I_{tr}) was obtained. Another glass plate was used as a standard for all the UVV experiments. All the photon transmission measurements were carried out at room temperature.

The variation of fluorescence emission of the composite films was measured by using Varian Carry Eclipse Fluorescence Spectrophotometer. Excitation and emission wavelengths were used as 370 and 507 nm, respectively. The emission wavelength at maximum intensity of pyranine is 510 nm, which varies up to 5–10 nm depending on the structure of the polymer molecules. The fluorescence emission measurements were performed at six different positions on the film surface in order to lower the error level, and the average value of the fluorescence emission intensity (I_{fl}) at the maximum was obtained.

The electrical resistivities of the PVAc/MWCNT composite films were measured by alternating polarity method with a Keithley Model 6517A electrometer which employs the ASTM D-257 measurement standard, and a test fixture which was reconstructed as three times minimized version of Keithley Model 8009 resistivity test fixture. The composite films were placed in the text fixture which have disk-shaped electrodes, then their surface resistivities, ρ_s (Ohm/square or Ohm) were measured under 10–100 V DC potential with alternating polarities for every 15-s period. All the surface resistivities of the composite films were determined for four different orientations and measurements were repeated many times in order to lower the error in the surface resistivity measurements. The average values obtained from the proper measurements were used to plot the graphics. A photo of the miniaturized text fixture and the experimental setup are shown in Figure 2.

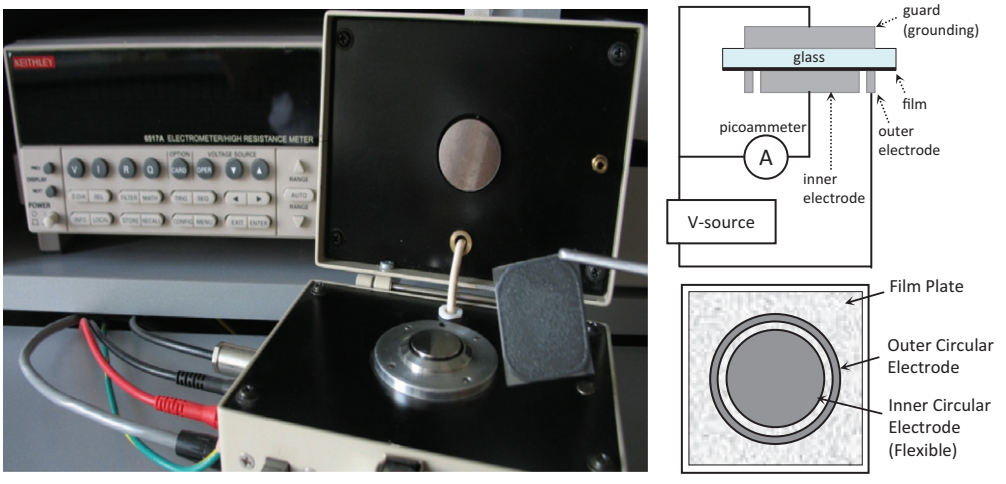

Figure 2. The photo of the miniaturized text fixture and the experimental setup.

3. Results and discussion

3.1. *Electrical percolation of MWCNTs*

The average values of the surface resistivities, ρ_s of PVAc/MWCNT composite films *versus* mass fractions of MWCNT, M were measured and observed that the surface resistivities (ρ_s) of the composite films do not change much below 1.0 wt% ($M \leq 1.0$ wt%). However, ρ_s values of the composite films dramatically decrease from 10^{11} Ohm/square to 10^4 Ohm/square in the band-gap of $M = 1.0$–4.0 wt%. This behavior indicates that the electrical percolation occurs at low levels of M. The surface conductivity values were calculated from the following equation.

$$\sigma = 1/\rho_s \tag{2}$$

The obtained results using Equation (2) are presented in Figure 3, where it can be seen that, the surface conductivity, σ starts to increase at the $M_\sigma = 1.0$ wt% by addition of MWCNT into the insulating PVAc matrix. This sudden increase can be interpreted by consisting of connected conductive paths of MWCNTs in the composite film. Thus, at this critical point the insulating system starts to transform to a more conductive state, which indicates that the percolation threshold of the surface conductivity (M_σ) is 1.0 wt%. The classical percolation theory can be used with the following equation above the critical point ($M > M_\sigma$) for the composite structure [8]:

$$\sigma = \sigma_o (M - M_\sigma)^{\beta_\sigma}, \tag{3}$$

where σ is the surface conductivity (Siemens/square), M is the volume or mass fraction of MWCNT, M_σ is the percolation threshold value, β_σ is the critical exponent for the surface conductivity, and σ_o is a scaling factor that may be comparable to the effective conductivity of pure MWCNT film [28,29]. β_σ was calculated from the slope of the curve in Figure 4 which was drawn from the logarithms of the surface conductivity data treated with Equation (3), and found to be as 2.1. The critical exponents calculated theoretically for 3D network systems were found to be in between 1.6 and 2.0, and experimentally produced β_σ values vary from 1.3 to 3.1 [30]. Here, the produced $\beta_\sigma = 2.1$ value is well agreed with the theoretical and the experimental results in the literature.

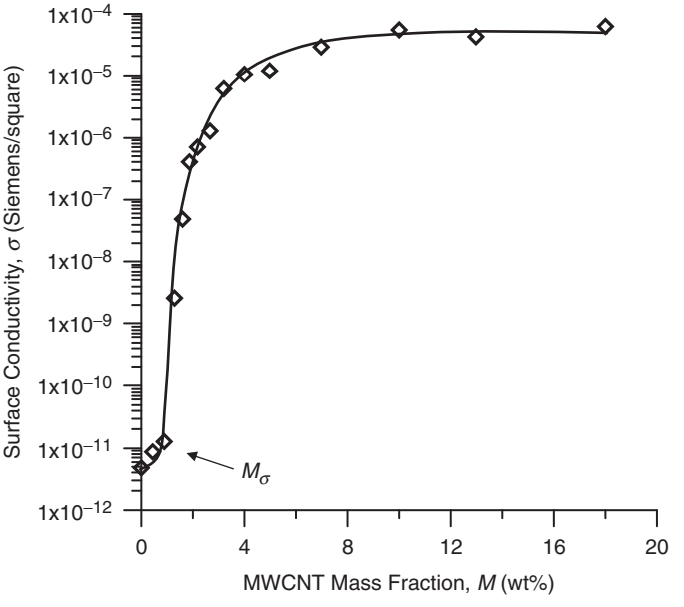

Figure 3. The surface conductivities, σ of PVAc/MWCNT composite films *versus* mass fractions of MWCNT, M.

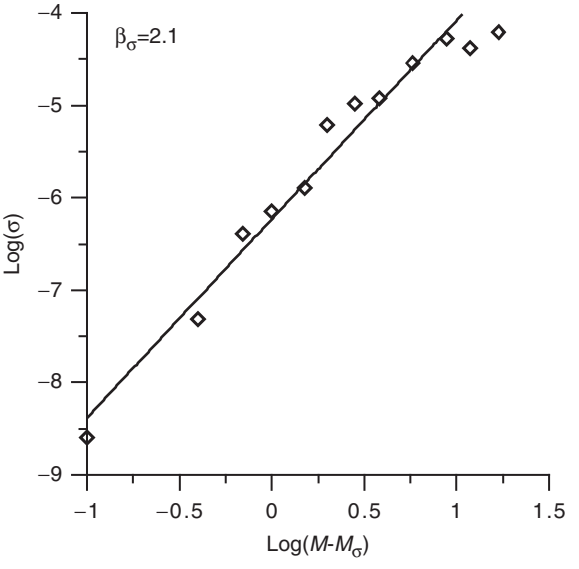

Figure 4. The log–log plot of σ *versus* $M - M_\sigma$. The slope of the straight line produces the electrical critical exponent, β_σ as 2.1.

On the other hand, in an experimental study performed by Choi et al. [1], volume resistivities of PVAc/MWCNT composites were found to be 3.7×10^{13}, 2.0×10^{13}, and $3.44 \times 10^{7}\,\Omega\,\mathrm{cm}$ for the MWCNT concentrations of 0, 0.1, and 0.5 wt%, respectively. Francis et al. [17] showed that the electrical percolation occurs in the range

from 0 to 2 vol% for SWCNT/PVAc composite systems. As a result of electrical conductivity measurements which are done in a similar composite system, the volume conductivity was raised to $10^{-1}\,S\,cm^{-1}$ by the addition of 0.04 wt% SWCNT, and the critical exponent was found as $\beta = 1.9$ [18]. Conductivity measurements for the composites of monodisperse and polydisperse latex and CB particles performed by Grunlan et al. [19] showed that the percolation point was around 2 vol% CB concentration [19]. In the same study, the critical exponent values for the samples which were dried at different temperatures were calculated in the intervals of 1.4 ± 0.4–2.2 ± 0.8 and 1.7 ± 0.4–2.6 ± 0.4, respectively. Our results are well agreed with the data of similar systems in the literature.

3.2. *Optical percolation of MWCNTs*

Transparency variations of the composite films *versus* mass fractions (M) of MWCNT were monitored by transmitted light intensity, I_{tr} from the films. It was observed that I_{tr} sharply decreases as MWCNT content increases in the composite system, and there is almost no light transmission from the films above the mass fraction of 7.0 wt% ($M \geq 7.0$ wt%). The decrease in the I_{tr} can be explained by the distribution of MWCNTs among the homogeneously dispersed PVAc chains, i.e., two medium with different refractive indices are randomly formed in the composite system. The scattering centers in the composite film are increased as M is increased, thus, more light is scattered and, as a result, the optical transmission of the film is decreased.

The behavior of I_{tr} *versus* M predicts that the composite system owns a percolative structure having a percolation threshold at 0.5 wt% MWCNT content. Previous experimental studies by others have shown that the rheological percolation threshold was lower than the electrical percolation threshold in some conductive polymeric composites. Du et al. [31] determined the electrical and rheological percolation thresholds for PMMA/SWCNT composite system as $m_{c\sigma} = 0.39$ and $m_{cG'} = 0.12\%$, respectively. Furthermore, they found that the critical exponents for the electrical and rheological measurements as $\beta_\sigma = 2.3$ and $\beta_{G'} = 0.7$, respectively. Another experimental study performed by using electrical, viscosity, and modulus measurement techniques on PET/MWCNT composite system, in where the percolation thresholds and the critical exponents were found to be as $m_{c,\sigma} = 0.009$, $m_{c,\eta} = 0.006$, $m_{c,G'} = 0.005$ and $\beta_{c,\sigma} = 2.2$, $\beta_{c,\eta} = 1.3$, $\beta_{c,G'} = 1.5$, respectively [32].

Here, the produced optical transmission data can be treated by employing the site percolation theory, where sites in a lattice are either filled or empty. Extended simulations and theoretical works have shown that the percolation probability is given as

$$P_\infty(p) \propto (p - p_c)^\beta. \tag{4}$$

If we assume that M is identical to lattice occupation probability, p, then the percolation threshold value, p_c will be equivalent to M_{op}. One can arrange the percolation equation (Equation (4)) for the optical data as follows:

$$I_{sc}(M) = I_o(M - M_{op})^{\beta_{op}}, \tag{5}$$

where the percolation probability, $P_\infty(p)$ is assumed to be proportional to the scattered light intensity $I_{sc} = I_o - I_{tr}$. Here, M represents the lattice occupation probability of MWCNTs in the PVAc matrix and M_{op} is its critical threshold value. Here, I_o is the incident light intensity. As M is increased, the scattered light intensity, I_{sc} increases due to the concentration fluctuations. Figure 5 shows the variation of I_{sc} *versus* mass fraction of

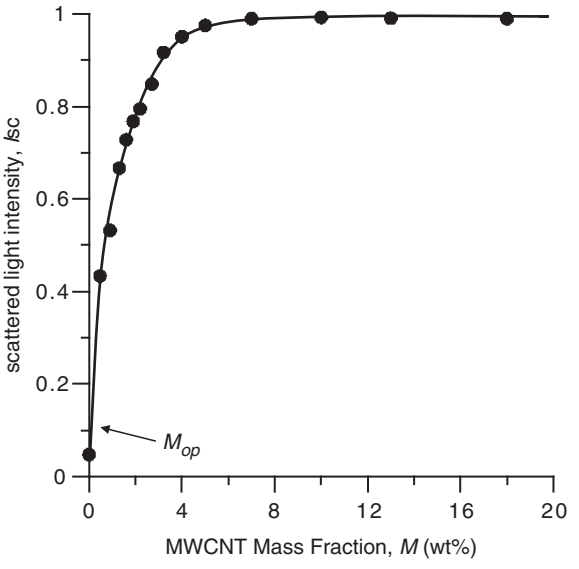

Figure 5. The scattered light intensity, I_{sc} *versus* MWCNT mass fraction, M.

MWCNT, M where the scattered light intensity increases rapidly, even though the MWCNT content was 0.5 wt% at the beginning which shows the percolation threshold value is in between 0 and 0.5 wt%. Since $M - M_{op} \rightarrow M$ for the extremely low M_{op} values, then Equation (5) can be written as

$$I_{sc}(M) = I_o M^{\beta_{op}} \tag{6}$$

The variation of log I_{sc}/I_o *versus* log M is given in Figure 6. The critical exponent, β_{op} was calculated as 0.40 from the slope of the straight line in Figure 6, using Equation (6). The obtained value of $\beta_{op} = 0.40$ is not far from the theoretical site percolation value of 0.42 [8]. The difference can be originated from the conditions of sample preparation and the experimental techniques that we have used.

3.3. *Fluorescence results of percolative MWCNTs*

A typical fluorescence emission spectra of pyranine from the composite films for various MWCNT content are presented in Figure 7, where it is seen that as MWCN content is increased, fluorescence intensity decreases. The maxima of the emission intensity (I_{fl}) *versus* mass fractions (M) of the samples are shown in Figure 8, where it can be seen that the emission intensities of pyranine show a rapid decrease for further addition of MWCNTs in the composite films. This behavior indicates that the percolation threshold M_{fl} is around 0–0.5 wt% for the fluorescence emission intensity measurements. Nevertheless, it seems that the emission intensity does not effectively change above 10 wt%, and the percolation occurs in the band gap of 0–10 wt%. As the MWCNT concentration is increased, the number of the scattering centers in the film also increases. As a result, the number of the photons which penetrate into the film and encounter the

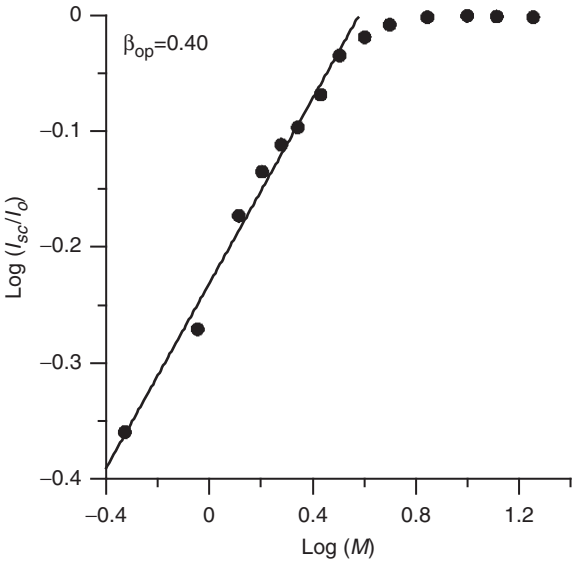

Figure 6. The log–log plot of I_{sc} *versus* M. The slope of the straight line produces the optical critical exponent, β_{op} as 0.40.

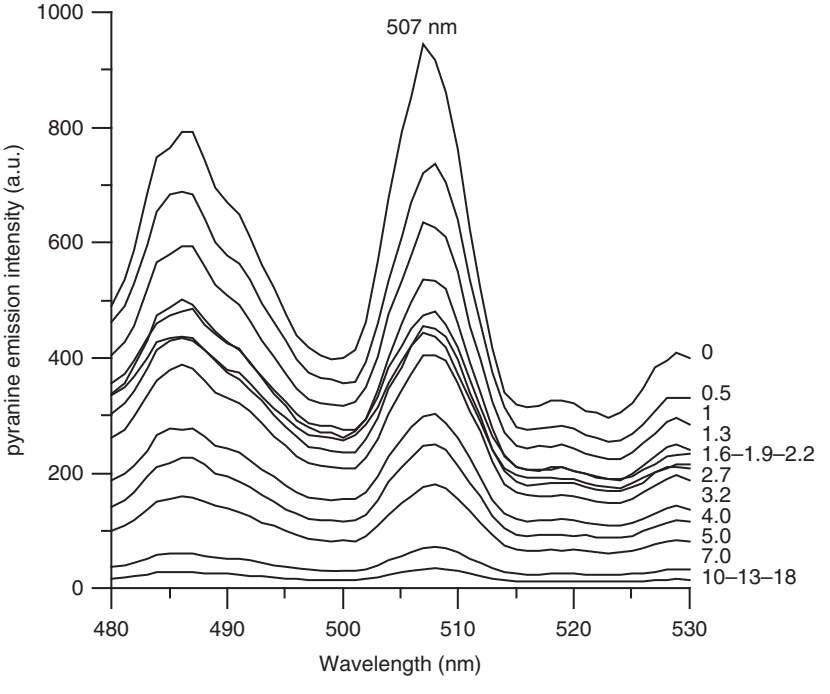

Figure 7. The fluorescence spectra of pyranine from PVAc/MWCNT composite film samples. The numbers near the curves are the mass fractions, M of the samples.

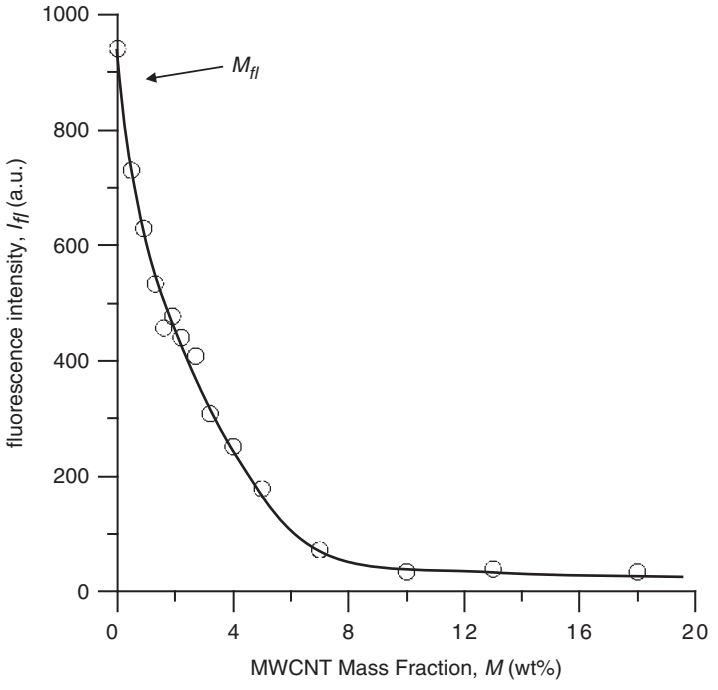

Figure 8. The fluorescence emission intensity, I_{fl} *versus* MWCNT mass fraction, M.

pyranine molecules dramatically decreases, which causes a decrease in the fluorescence emission intensity, I_{fl}.

The fluorescence emission data in Figure 8 can be treated by the percolation theory. If one assumes that M is identical to lattice occupation probability, p, then the percolation threshold value, p_{c} will be equivalent to M_{fl}, then Equation (4) could be arranged as

$$\frac{1}{I_{\mathrm{fl}}} = (M - M_{\mathrm{fl}})^{\beta_{\mathrm{fl}}} \tag{7}$$

Since $(M - M_{\mathrm{fl}}) \rightarrow M$ for low M_{fl} then Equation (7) becomes as follows

$$\frac{1}{I_{\mathrm{fl}}} = M^{\beta_{\mathrm{fl}}} \tag{8}$$

by assuming the percolation probability $P_{\infty}(p)$ is inversely proportional to the fluorescence emission intensity. The variation of $\log(1/I_{\mathrm{fl}}) - \log(M)$ is presented in Figure 9 where two different percolation regions can be detected. The critical exponents, β_{fl} was calculated and found to be as 0.35 and 2.0 from the slopes of the straight lines in Figure 9, according to Equation (8). The produced β_{fl} value for low MWCNT content region provides the site percolation value of 0.35. However, at high MWCNT content region β_{fl} value (2.0) is quite compatible with the electrical critical exponent $\beta_{\sigma} = 2.1$, and also with its theoretical value which is equal to 2. These results can be explained by assuming that the pyranine molecules concentrate around the MWCNTs during the preparation of the composite film. As a result, the photons penetrating into the film encounter with the MWCNTs several times and interact with the pyranine molecules and excite them to emit the fluorescence

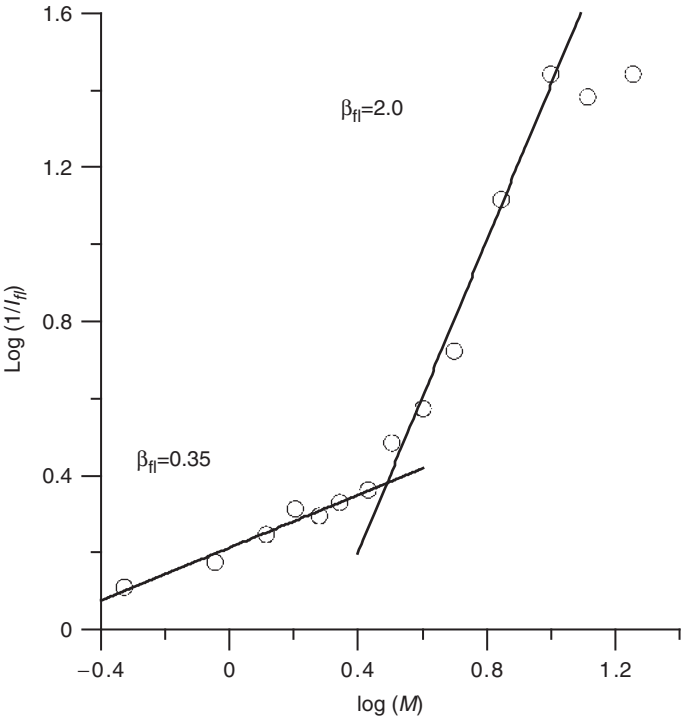

Figure 9. The log–log plot of $1/I_{\mathrm{fl}}$ *versus* M. The slopes of the straight lines produce the fluorescence critical exponents, β_{fl} as 0.35 and 2.0 for the low and high MWCNT concentration regions, respectively.

light at 507 nm. At low MWCNT content, pyranine simply probes the scattering sites in the composite film, however at high MWCNT concentration, pyranine now traces the conducting network. In other words, the pyranine molecules trace the MWCNT sites and produces the similar critical exponents in two regions. In the low MWCNT concentration region, I_{fl} starts to decrease by following the increase in the number of scattering centers in the structure, showing a similar intensity behavior to that of the optical I_{tr} data. In the high MWCNT region, the formation of the conductive paths from MWCNTs, which are covered by the pyranine molecules improves the surface conductivity by carrying out information about the fluorescence response of the film structure.

The differences between the electrical, optical and fluorescence percolation processes and the behaviors of the composite systems are represented in Figure 10. In Figure 10(a), for the pure PVAc film, the conductivity is extremely low, and the optical transmission and the fluorescence emission are quite high for this film. Figure 10(b) represents the optical, electrical, and fluorescence behaviors for the films with low MWCNT. While the optical transmittance is decreased due to the existence of MWCNTs (existence of different refractive mediums), the scattered light intensity increases. Since the photons start to be scattered from the film surface, the penetration of the photons and their interaction with the pyranine molecules are obstructed. Thus, the fluorescence emission intensity also starts to decrease. As far as the electrical conductivity is concern, immediately above the critical point ($M > M_{\sigma}$) up to $M = 4$ wt% content, tunneling and/or hopping of electrons played the important role in conductivity. The tunneling distance allowed for electron hopping

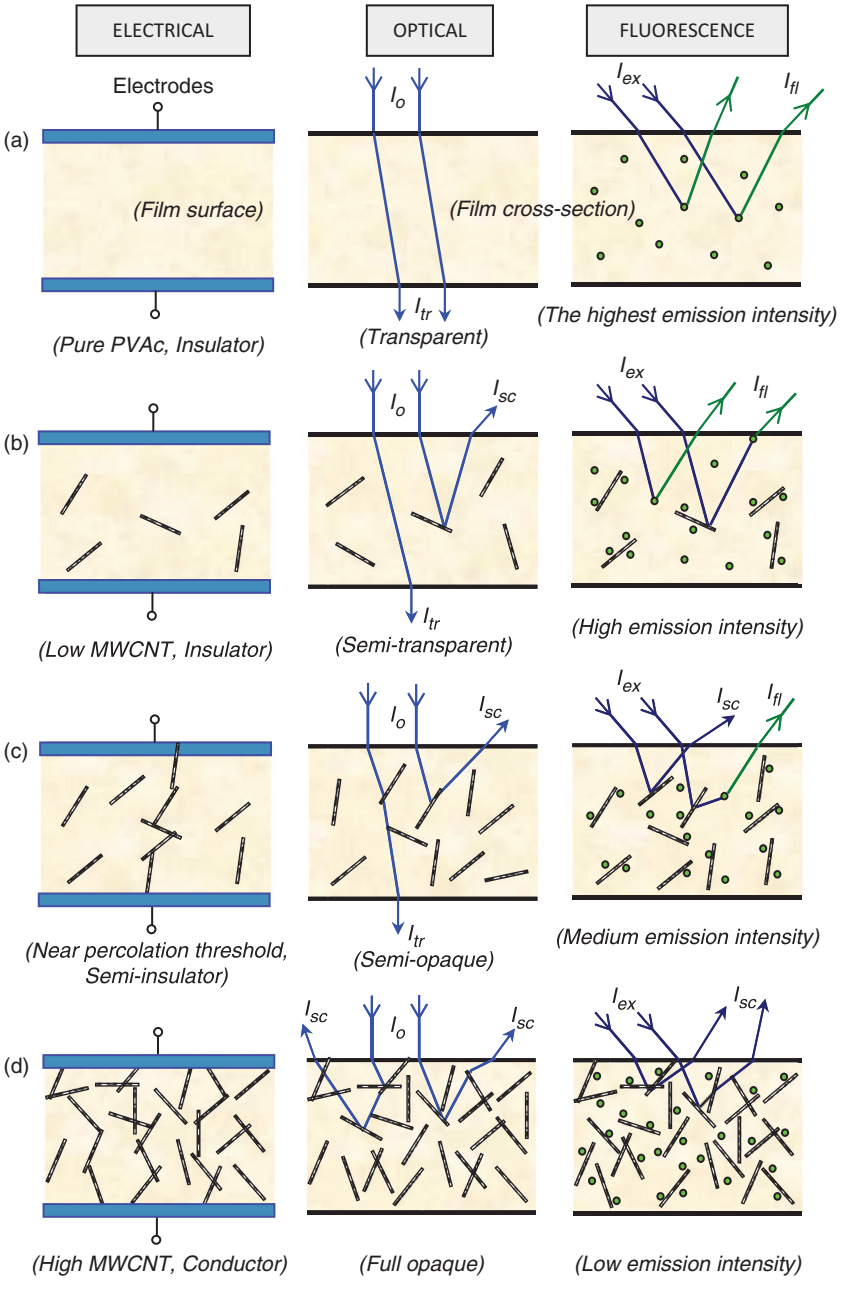

Figure 10. A cartoon representation of electrical, optical and fluorescence percolation processes depending on the MWCNT concentration.

has been reported between 5 and 30 nm [31,33–35]. However, above 4 wt%, interconnected network starts to form and MWCNT network is completed at the saturation level of CNTs above 10 wt%. In this picture, optical and fluorescence exponents are similar by obeying site percolation model. In the composites which have high enough MWCNT

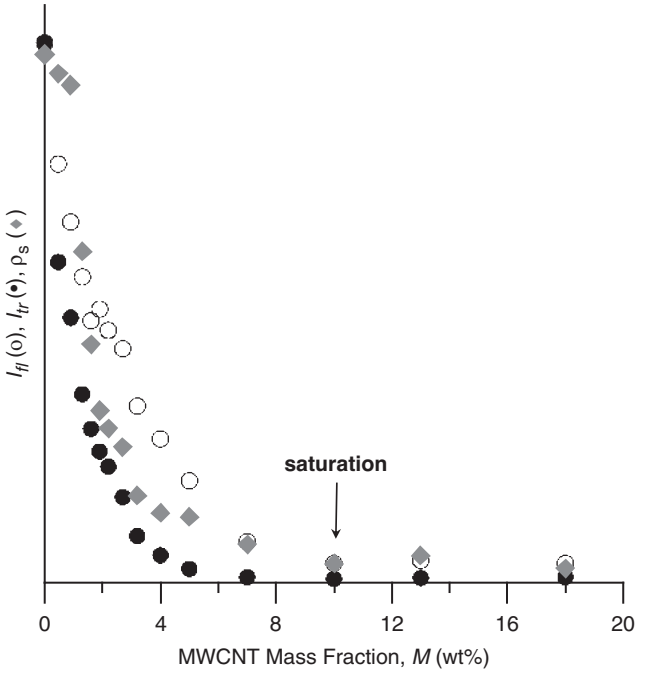

Figure 11. The comparison of the data obtained from electrical (ρ_s), optical (I_{tr}), and fluorescence (I_{fl}) measurements.

concentrations the electrical conduction starts as shown in Figure 10(c). At this concentration level, some conductive paths start to form, resulting the increase in conductivity. Here, pyranine molecules probe the conductivity path. The optical transmittance and the fluorescence emission continue to decrease due to increase in the number of MWCNTs acting as scattering centers in the film. Above the electrical percolation threshold, the composite system becomes as in Figure 10(d). The MWCNTs starts to form many conductive paths and as a result, the electrical conductivity sharply increases. However, the composite film scatters high number of photons due to increase in the heterogeneity level of the film. Thus, the optical transmittance and fluorescence emission levels become quite low due to obstruction of penetrating photons into the composite film. The produced data from these three different monitoring techniques are compared in Figure 11. Even though the percolation thresholds are quite different, the saturation points are almost the same for three measurement systems (~10 wt%).

4. Conclusion

This study has shown that the insulator-conductor transition takes place by the addition of a small amount of MWCNT to the composite system. Surface resistivity (ρ_s) of the composite films dramatically decrease from 10^{11} to 10^4 Ohm/square in the band-gap of $M = 1.0$–4.0 wt%. The insulator system starts to transform to a more conductive state by consisting of conductive paths of MWCNTs between the electrodes. The size of MWCNTs and electron hopping and/or tunneling effects play important roles in the early percolation

behavior of the films. Nano/micro-size of MWCNT plays a fundamental role for the scattering of light from the composite film. In other words, inclusion of very small amount of CNT scatters light dramatically. As a result, the optical transparency shows a very low percolation threshold. The fluorescence emission intensity, I_{fl} decreases as MWCNT concentration is increased, i.e., scattering centers in the film are increased as the mass fraction, M is increased. Thus, the number of the photons which 'encounter' with pyranine molecules decreases in parallel with the number of photons penetrating into the film.

In the current work, the conductivity, optical and fluorescence percolation thresholds and the critical exponents were determined and found to be as $M_\sigma = 1.0\,\text{wt\%}$, $M_{op} = 0\text{–}0.5\,\text{wt\%}$, $M_{fl} = 0\text{–}0.5\,\text{wt\%}$ and $\beta_\sigma = 2.1$, $\beta_{op} = 0.40$, $\beta_{fl} = 0.35$ and 2.0, respectively. The critical exponent values of electrical and fluorescence percolations were found to be higher than that of optical percolation at high MWCNT region, where the characteristics in fluorescence and electrical curves have similar behaviors and similar critical exponents as contrary to the optical data. This prediction can be used to roughly follow the conductivity of such composite films by using fluorescence data. On the other hand at low MWCNT region fluorescence percolation imitates optical percolation producing the similar critical exponents.

Acknowledgments

The authors thank Prof. Ayfer Sarac et al. for synthesizing and providing the PVAc latex material.

References

[1] Choi CS, Park BJ, Choi HJ. Electrical and rheological characteristics of poly(vinyl acetate)/multi-walled carbon nanotube nanocomposites. Diam Relat Mater. 2007;16:1170–1173.
[2] Verma SK, Bisarya SC. Improvement in properties of poly(vinyl acetate)-emulsion with dibasic acids. J Appl Polym Sci. 1986;31:2675–2684.
[3] Sung JH, Park SJ, Park JH, Choi HJ, Choi JS. Characteristics of poly(vinyl acetate) as a gate insulating material in organic thin film transistors. Synthetic Met. 2006;156:861–864.
[4] Lovell PA, El-Aasser MS. Emulsion polymerization and emulsion polymers. Chichester: John Wiley and Sons; 1997.
[5] El-Aasser MS, Vanderhoff JW. Emulsion polymerization of vinyl acetate. London and New Jersey: Applied Science Publication; 1981.
[6] Ajayan PM, Stephan O, Colliex C, Trauth D. Aligned carbon nanotubes in a thin polymer film. Science. 1994;265:1212–1214.
[7] Ajayan PM, Zhou OZ. Applications of carbon nanotubes. Top Appl Phys. 2001;80:391–425.
[8] Stauffer D, Aharony A. Introduction to percolation theory. London: Taylor & Francis; 1994.
[9] Bauhofer W, Kovacs JZ. A review and analysis of electrical percolation in carbon nanotube polymer composites. Compos Sci Technol. 2009;69:1486–1498.
[10] Gao L, Zhou X, Ding Y. Effective thermal and electrical conductivity of carbon nanotube composites. Chem Phys Lett. 2007;434:297–300.
[11] Du F, Scogna RC, Zhou W, Brand S, Fischer JE, Winey KI. Nanotube networks in polymer nanocomposites: Rheology and electrical conductivity. Macromolecules. 2004;37:9048–9055.
[12] Wang G, Tan Z, Liu X, Chawda S, Koo JS, Samuilov V, Dudley M. Conducting MWNT/poly(vinyl acetate) composite nanofibres by electrospinning. Nanotechnology. 2006;17:5829–5835.

[13] Miriyala SM, Kim YS, Liu L, Grunlan JC. Segregated networks of carbon black in poly(vinyl acetate) latex: influence of clay on the electrical and mechanical behavior. Macromol Chem Phys. 2008;209:2399–2409.
[14] Yu C, Kim YS, Kim D, Grunlan JC. Thermoelectric behavior of segregated-network polymer nanocomposites. Nano Lett. 2008;8:4428–4432.
[15] Moriary GP, Wheeler JN, Yu C, Grunlan JC. Increasing the thermoelectric power factor of polymer composites using a semiconducting stabilizer for carbon nanotubes. Carbon. 2012;50:885–895.
[16] Kim YS, Kim D, Martin KJ, Yu C, Grunlan JC. Influence of stabilizer concentration on transport behavior and thermopower of CNT-filled latex-based composites. Macromol Mater Eng. 2010;295:431–436.
[17] Francis LF, Grunlan JC, Sun J, Gerberich WW. Conductive coatings and composites from latex-based dispersions. Colloid Surface A. 2007;311:48–54.
[18] Grunlan JC, Mehrabi AR, Bannon MV, Bahr JL. Water-based single-walled-nanotube-filled polymer composite with an exceptionally low percolation threshold. Adv Mater. 2004;16:150–152.
[19] Grunlan JC, Gerberich WW, Francis LF. Electrical and mechanical behavior of carbon black-filled poly(vinyl acetate) latex-based composites. Polym Eng Sci. 2001;41:1947–1962.
[20] Kara S, Pekcan Ö, Sarac A, Arda E. Film formation stages for poly(vinyl acetate) latex particles: a photon transmission study. Colloid Polym Sci. 2006;284:1097–1105.
[21] Arda E, Kara S, Pekcan Ö. A photon transmission study for film formation from poly(vinyl acetate) latex particles with different molecular weights. J Polym Sci Pol Phys. 2007;45:2918–2925.
[22] Arda E, Kara S, Pekcan Ö. Effect of annealing rate on film formation from poly(vinyl acetate) latex particles. Compos Interf. 2008;15:19–33.
[23] Kara S, Arda E, Dolastir F, Pekcan Ö. Electrical and optical percolations of polystyrene latex-multiwalled carbon nanotube composites. J Colloid Interf Sci. 2010;344:395–401.
[24] Sarac A. Semicontinuous emulsion copolymerization of vinyl acetate and butyl acrylate using different initiators and different chain length emulsifiers. Macromol Symp. 2004;217:161–167.
[25] Vaisman L, Wagner HD, Marom G. The role of surfactants in dispersion of carbon nanotubes. Adv Colloid Interf. 2006;128:37–46.
[26] O'Connell MJ, Boul P, Ericson LM, Huffman C, Wang YH, Haroz E, Kuper C, Tour J, Ausman KD, Smalley RE. Reversible water-solubilization of single-walled carbon nanotubes by polymer wrapping. Chem Phys Lett. 2001;342:265–271.
[27] Manivannan S, Jeong IO, Ryu JH, Lee CS, Kim KS, Jang J, Park KC. Dispersion of single-walled carbon nanotubes in aqueous and organic solvents through a polymer wrapping functionalization. J Mater Sci Mater Electron. 2009;20:223–229.
[28] Hernández JJ, García-Gutiérrez MC, Nogales A, Rueda DR, Kwiatkowsa M, Szymczyk A, Roslaniecb Z, Conchesoc A, Guineac I, Ezquerra TA. Influence of preparation procedure on the conductivity and transparency of SWCNT-polymer nanocomposites. Compos Sci Technol. 2009;69:1867–1872.
[29] Chang L, Friedrich K, Yeand L, Toro P. Evaluation and visualization of the percolating networks in multiwall carbon nanotube/epoxy composites. J Mater Sci. 2009;44:4003–4012.
[30] Weber M, Kamal MR. Estimation of the volume resistivity of electrically conductive composites. Polym Compos. 1997;18:711–725.
[31] Du F, Scogna RC, Zhou W, Brand S, Fischer JE, Winey KI. Nanotube networks in polymer nanocomposites: rheology and electrical conductivity. Macromolecules. 2004;37:9048–9055.
[32] Hu G, Zhao C, Zhang S, Yang M, Wang Z. Low percolation thresholds of electrical conductivity and rheology in poly(ethylene terephthalate) through the networks of multi-walled carbon nanotubes. Polymer. 2006;47:480–488.
[33] Li J, Ma PC, Chow WS, To CK, Tang BZ, Kim J-K. Correlations between percolation threshold, dispersion state, and aspect ratio of carbon nanotubes. Adv Funct Mater. 2007;17:3207–3215.

[34] Du F, Guthy C, Kashiwagi T, Fischer JE, Winey KI. An infiltration method for preparing single-wall nanotube/epoxy composites with improved thermal conductivity. J Polym Sci B Pol Phys. 2006;44:1513–1519.
[35] Seidel GD, Lagoudas DC. A micromechanics model for the electrical conductivity of nanotube-polymer nanocomposites. J Compos Mater. 2009;43:917–941.